

CHEMISTRY

A European Journal



Accepted Article

Title: Spectroscopy and Reactivity of Dialkoxy Acenes

Authors: Valentina Brega, Sare Nur Kanari, Connor T. Doherty, Dante Che, Seth A. Sharber, and Samuel William Thomas

This manuscript has been accepted after peer review and appears as an Accepted Article online prior to editing, proofing, and formal publication of the final Version of Record (VoR). This work is currently citable by using the Digital Object Identifier (DOI) given below. The VoR will be published online in Early View as soon as possible and may be different to this Accepted Article as a result of editing. Readers should obtain the VoR from the journal website shown below when it is published to ensure accuracy of information. The authors are responsible for the content of this Accepted Article.

To be cited as: *Chem. Eur. J.* 10.1002/chem.201901258

Link to VoR: <http://dx.doi.org/10.1002/chem.201901258>

Supported by
ACES

WILEY-VCH

Spectroscopy and Reactivity of Dialkoxy Acenes

Valentina Brega,^[a] Sare Nur Kanari,^[a] Connor T. Doherty,^[a] Dante Che,^[a] Seth A. Sharber,^[a] and Samuel W. Thomas III^{*[a]}

Abstract: Photochemical oxidation of acenes can benefit or impede their function, depending on the application. Although acenes with alkoxy substituents on reactive sites are important for applications as diverse as drug delivery and organic optoelectronics, the influence of chemical structure on their photochemical oxidation remains unknown. This paper therefore describes the synthesis, spectroscopic properties, and reactivity with singlet oxygen ($^1\text{O}_2$) of a series of dialkoxyacenes that vary in the number and types of fused rings in the (hetero)acene cores. Reductive alkylation of quinone precursors yielded target dialkoxyacenes with fused backbones ranging from benzodithiophene to tetracenothiophene. Trends of their experimental spectroscopic characteristics were consistent with time-dependent density functional theory (TD-DFT) calculations. NMR studies show that photochemically generated $^1\text{O}_2$ oxidizes all but one of these acenes to the corresponding endoperoxides in organic solvent. The rates of these oxidations correlate with the number and types of fused arenes, with longer dialkoxyacenes generally oxidizing faster than shorter derivatives. Finally, irradiation of these acenes in acidic, oxidizing environments cleaves the ether bonds. This work impacts those working in organic optoelectronics, as well as those interested in harnessing photogenerated reactive oxygen species in functional materials.

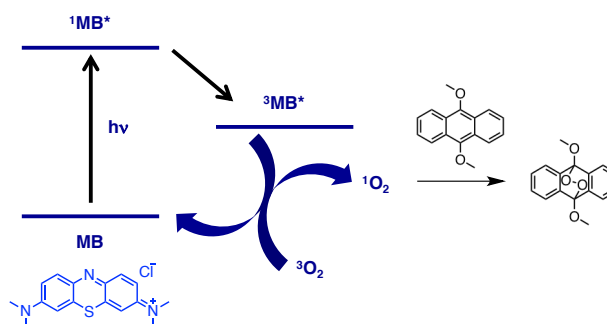
Introduction

Acenes occupy a central position in physical organic chemistry and a wide range of functional materials. Some applications, such as organic field effect transistors (OFETs)^[1] and organic light emitting devices (OLEDs),^[2] require compounds that resist chemical reactivity and unwanted degradation. Beyond fully carbocyclic fused rings, heteroacenes such as thienoacenes and azaacenes offer increased tunability of crystal packing, electronic structure, optoelectronics, and reactivity for all the above applications. Within the large family of acene- and heteroacene-based organic optoelectronics, small molecules and conjugated polymers comprising dialkoxyacenes, especially heteroacene derivatives such as benzodithiophene and anthradithiophene, have figured prominently in these applications.^[3]

On the other hand, the unique and relatively predictable

chemical reactivity of acenes, especially in [4+2] or photoinduced [4+4] “butterfly” dimerization reactions,^[4] has spearheaded innovations in dynamic covalent chemistry and photo-responsive molecules.^[5] Among these reactions, [4+2] cycloadditions with the lowest energy electronic excited state of O_2 —singlet oxygen ($^1\text{O}_2$)—to form endoperoxides are especially relevant. Although photochemical endoperoxidation degrades acenes for optoelectronic materials by disrupting the conjugated cores of acenes, acene endoperoxide formation constitutes the basis of probes for $^1\text{O}_2$,^[6] such as the commercially available Singlet Oxygen Sensor Green. These probes function through endoperoxidation widening the gap between frontier molecular orbitals of the acene, therefore impacting the intensity or energy of observed luminescence. Recently, our group has used acenes as energy acceptors in conjugated polymer nanoparticles (CPNs) for ratiometric fluorescence responses to $^1\text{O}_2$.^[7]

Beyond their role as the primary reaction products in reactions between acenes and $^1\text{O}_2$, the reactions of endoperoxides themselves present unique opportunities.^[8] Endoperoxide cycloreversion can occur in some cases to reconstitute acenes,^[9] which not only enables recovery from oxidation-induced damage to acene-based optoelectronic materials, but also presents a novel approach for delivering cytotoxic reactive oxygen species.^[10] In contrast to these reversion reactions, alkoxyacene endoperoxides can undergo high-yielding endoperoxide decomposition pathways, in which the acetal-like linkages cleave to yield quinones and alcohols, which is useful for photooxidative cleavage of covalent bonds.^[11]



Scheme 1. Photooxidation of 9,10-dimethoxyanthracene using methylene blue (MB) as a photosensitizer.

[a] Dr. V. Brega, S. N. Kanari, C. T. Doherty, D. Che, S. A. Sharber, Prof. S. W. Thomas III
Department of Chemistry
Tufts University
62 Talbot Avenue, Medford MA 02155, United States
E-mail: sam.thomas@tufts.edu

Supporting information for this article is given via a link at the end of the document

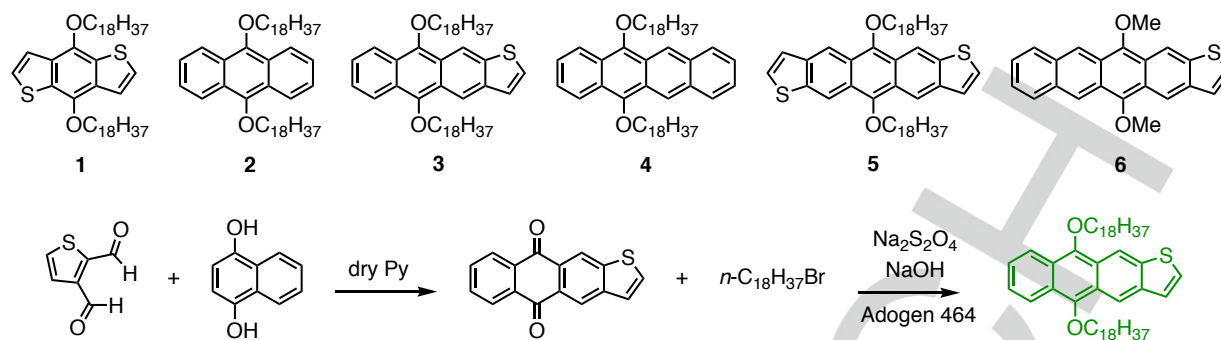


Figure 1. Top: Structures of dialkoxyacenes 1-6. Bottom: Example synthesis, here of thienoanthracene 3.

Given the potential utility of alkoxyacenes, a systematic, quantitative understanding of how their chemical structures influence spectroscopic properties and reactivity with $^1\text{O}_2$ impacts fundamental and applied chemistry. Available literature reports, to the best of our knowledge, assess these properties mainly for derivatives of three or fewer fused rings, with few exceptions. For example, 9,10-dimethoxyanthracene has a cycloaddition rate constant with $^1\text{O}_2$ of $1.4 \times 10^7 \text{ M}^{-1}\text{s}^{-1}$ —about one order of magnitude larger than the commonly used reactivity standard 9,10-diphenylanthracene.^[12] Similar oxidations of naphthalene analogs are relatively slow ($k \sim 10^4\text{-}10^5 \text{ M}^{-1}\text{s}^{-1}$), while the corresponding endoperoxides fragment at room temperature. Aubry and coworkers used a 1,4-dialkoxyanthracene core to construct water-soluble, $^1\text{O}_2$ -reactive naphthalenes,^[13] while Linker and coworkers isolated and characterized the thermally labile endoperoxides of 1,4-dialkoxyanthracenes, which form peroxy bridges on the dialkoxy ring selectively.^[14] With respect to longer acenes, Neckers and coworkers described highly substituted, photostable pentacenes and tetracenothiophenes that combine two ethynyl groups on the central ring of these compounds with two methoxy groups on an adjacent ring.^[15] Other insights have included dialkoxytetracene derivatives that undergo [4+4] photodimerizations,^[4b] and 6,13-dialkoxytetracenes with HOMO-LUMO gaps of $\sim 2.0\text{-}2.1 \text{ eV}$.^[16] Given the importance of acenes with more than three fused rings in optoelectronic devices, including their rapid reactivity with $^1\text{O}_2$, in addition to the unique influences of alkoxy groups on acene chemistry, our objective here is to understand the relationship between the chemical structures, spectroscopy, and reactivities of dialkoxyacenes.

Results and Discussion

Experimental Design and Synthesis

We designed a series of six dialkoxyacene analogs that vary in the number (three-five) and types (benzene or thiophene) of fused rings comprising the acene core, each with *n*-alkoxy chains. Consistent with well-documented trends in acene chemistry, we expected that longer acenes would react faster than shorter acenes. We also expected that addition of a fused thiophene ring to an existing acene core would have a smaller

impact on reactivity and spectroscopy than addition of an additional benzene ring, because the resonance energy of benzene (36 kcal/mol) is higher than that of thiophene (29 kcal/mol).^[17] Although the reactivity of most long acenes detracts from device stability and performance in electronics applications, highly reactive acenes can improve sensitivity of $^1\text{O}_2$ -responsive materials and offer faster chemical conversion in other applications that harness cycloaddition reactions. In addition to higher reactivity toward singlet oxygen, longer acenes generally offer red-shifted absorbance and emission spectra.

Syntheses of dialkoxyacenes involved reductive alkylation of the corresponding quinones in biphasic mixtures using a phase transfer catalyst, an alkylating agent, and sodium hydrosulfite as a reducing agent. In almost all cases, we alkylated these quinones with 1-bromooctadecane (Figure 1) to yield octadecyloxy-substituted acenes 1-5; preparation of 6 from tetracenomonothiophene (TMT) quinone required the stronger electrophile dimethyl sulfate. We note that anthradithiophene (ADT) 5 was isolated as a mixture of *syn* and *anti* isomers with respect to the terminal thiophene rings; previous reports indicate that the chemical properties of analogous stereoisomers of other ADT derivatives are nearly identical.^[18]

Optical Spectroscopy

Figure 2 shows the UV/vis absorbance spectra of dialkoxyacenes 1-5 in CH_2Cl_2 and 6 in THF, while Table 1 summarizes their photophysical parameters. The absorbance spectrum of each compound displays an intense absorbance band in the ultraviolet region and well-resolved vibronic peaks at longer wavelengths, with molar extinction coefficients between 7000 and $13000 \text{ M}^{-1}\text{cm}^{-1}$. Consistent with the increased conjugation of longer acenes, the lowest energy absorption maximum for these compounds (λ_{max}) shifts from 351 nm for benzodithiophene 1 to 560 nm for tetracenomonothiophene (TMT) 6. Addition of a fused thiophene ring (comparing 2 and 3, 3 and 5, or 4 and 6) yields comparatively small bathochromic shifts of 55-77 nm compared to addition of a fused benzene ring, which yields a shift of 120 nm when comparing 2 and 4, and 98 nm when comparing 3 and 6.

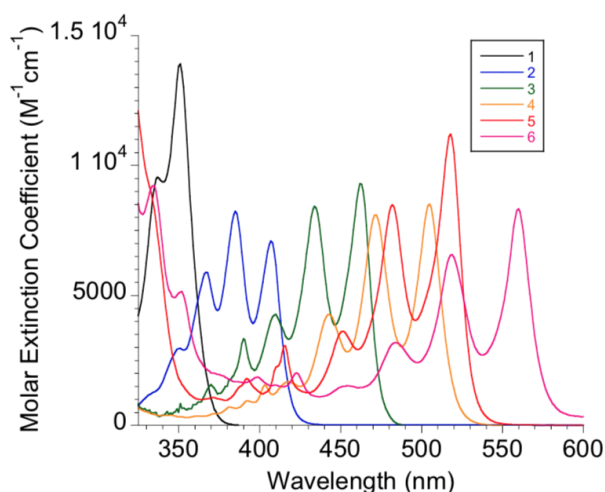


Figure 2. UV/Vis absorbance spectra of dialkoxyacenes **1-5** in CH_2Cl_2 and **6** in THF.

The absorbance spectra of each of these molecules are red-shifted relative to derivatives with identical fused ring cores but with diaryl substituents on the same positions of the acene, but blue-shifted relative to analogs with one aryethynyl and one aryl substituent on those positions.^[17] For example, the lowest energy absorbance maxima of 5,12-dioctyloxytetracene **4** (505 nm) lies between that of 5,12-dianisyltetracene (495 nm) and 5-anisyl-12-phenylethynyltetracene (523 nm). In fact, the shifts from the previously reported dianisyl derivatives to the dialkoxy derivatives here is consistently between 9 and 18 nm. Time-dependent density functional theory calculations for these molecules reflected this same trend, with **1** having the highest energy absorbance band, and **6** having the lowest energy absorbance.

Similar to the trend in absorbance spectra, the fluorescence emission spectra of these compounds shifted to lower energy with increasing number of fused aromatic rings, from 392 nm for benzodithiophene **1** to 577 nm for tetracenothiophene **6**. In addition, close correlation to known analogs also persists in the fluorescence spectra, with modest

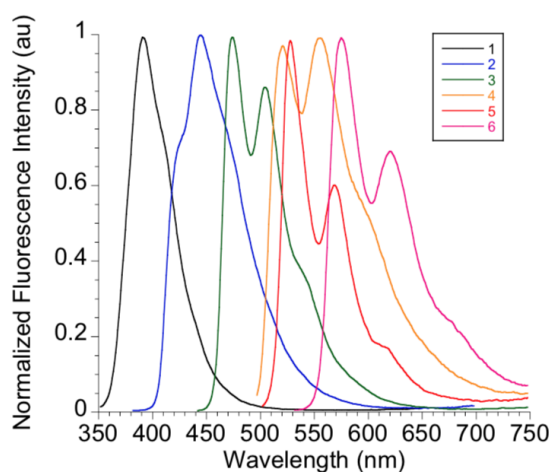


Figure 3. Height-normalized emission spectra of dialkoxyacenes **1-5** in CH_2Cl_2 and **6** in THF.

bathochromic shifts of the spectra of these compounds relative to dianisyl derivatives, ranging between 6 nm to 18 nm. Except for compound **1** ($\Phi_F = 0.11$), dialkoxyacenes **2-6** are efficient fluorophores ($\Phi_F > 0.4$), which is important for any prospective applications in fluorescent sensors or light emitting devices. Time resolved fluorescence of dialkoxyacenes **2-6** showed monoexponential decays with lifetimes longer than 10 ns. Together with the trends from UV/vis absorbance spectra, we conclude that with respect to the HOMO-LUMO gap and optical spectroscopy, addition of a fused thiophene to the terminus of an acene yields slightly more than half the shift of adding a fused benzene ring. The similarity of the spectral positions of compounds **4** and **5** exemplifies this guideline. This quantitative trend of comparing thiophene and benzene addition is similar to the trends of related modifications of diaryl, aryl-ethynyl, and diethynylacene.

Table 1. Spectroscopic parameters of **1-6**

Acene	$\lambda_{\text{max,abs}}$, nm	ϵ , $\text{M}^{-1}\text{cm}^{-1}$	$\lambda_{\text{max,fl}}$, nm ^[b]	Stokes Shifts, nm	Φ_F	τ , ns	$\lambda_{\text{max}}^{\text{cal}}$ [c]
1	351, ^[a] 255	13400	392	41	0.11	.. ^[d]	294
2	385, ^[a] 262	8300	445	60	0.91	10.2	349
3	462, ^[a] 278	9300	475	13	0.56	12.9	395
4	505, ^[a] 284	8300	522	50	0.49	12.7	435
5	518, ^[a] 301	11500	527	9	0.74	16.3	430
6	560, ^{[a],[e]} 303	7400 ^[e]	577 ^[e]	17	0.49 ^[e]	15.2	469

[a] Wavelength at which extinction coefficient was reported.

[b] For the (0,0) band.

[c] TD-DFT calculated.

[d] 403 nm pulsed LED used for TCSPC does not excite **1**

[e] In THF.

Endoperoxide formation

Due to the importance of dialkoxyacenes in photo-cleavable materials,^{[11a,c],[19]} as well as their potential utility in optoelectronic devices and in materials for luminescent response to $^1\text{O}_2$, a key objective is to understand how the structure of dialkoxyacenes influences their photochemical oxidation by $^1\text{O}_2$. To establish the structures of products formed upon exposure of these dialkoxyacenes to $^1\text{O}_2$, we irradiated CDCl_3 solutions of methylene blue (MB, ~0.6 mM) in the presence of acenes (~6 mM) at $\lambda > 630$ nm. Under these conditions, the acenes absorb no light, and any photoproducts occur through photosensitization of $^1\text{O}_2$ generated upon energy transfer from excited states of MB to O_2 . We chose CDCl_3 as a solvent because $^1\text{O}_2$ has an especially

long lifetime of 840 μs in CDCl_3 and its convenience for direct NMR analysis of products.^[20]

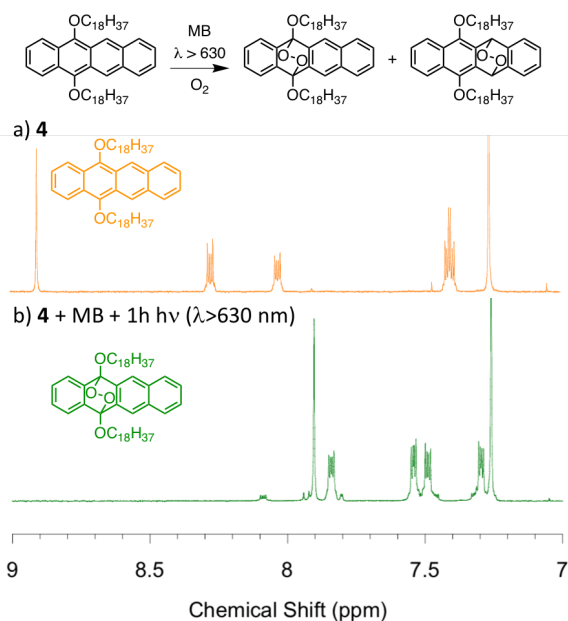


Figure 4. Aromatic region of ^1H NMR spectra in CDCl_3 of a) dialkoxytetracene **4** before and b) after one-hour irradiation at $\lambda > 630$ nm in the presence of MB.

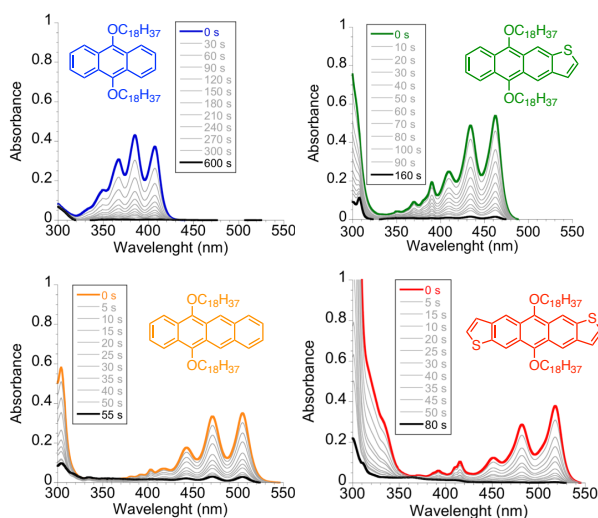


Figure 5. UV/vis response of **2**, **3**, **4**, and **5** to $^1\text{O}_2$ produced by photosensitization (solvent = CH_2Cl_2 , photosensitizer = methylene blue).

Dialkoxyacenes **2-5** reacted with $^1\text{O}_2$ to yield endoperoxides as major products. NMR analysis of the as-irradiated **2**, **3**, and **5** revealed one endoperoxide product, which in all cases corresponded to selective cycloaddition across the dialkoxyarene ring. The central carbocyclic rings of acenes are generally the most reactive, as the resulting products have the largest magnitude of aromatic stabilization. ^{13}C NMR spectra supported the formation of the endoperoxide across the electron-rich ring as a major product, for which a resonance at 102-103 ppm corresponds to the carbon connected to the endoperoxide bridge (Figure S14 and S17). In the case of **1**, NMR spectroscopy revealed no endoperoxide after one hour of irradiation, which highlights the stability of benzodithiophene derivatives that renders them useful in organic electronics.^[21]

In contrast to the other acene cores investigated here, unsubstituted tetracene has two equivalent central rings with potential to react as dienes. Therefore, when the central rings of tetracene derivatives are not identically substituted, the distribution of observed endoperoxide regioisomers gives direct comparisons of how substituents influence cycloaddition reactivity. Our previous work used this approach to elucidate steric and electronic substituent effects in endoperoxide formation.^[22] Here, exposing 5,12-dioctyloxyltetracene **4** to $^1\text{O}_2$ through irradiation of methylene blue in CDCl_3 yielded the expected two endoperoxides, with cycloaddition across the alkoxy-substituted ring as the major product in a 9:1 molar ratio (Figure 4 and Figure S16); the minor regioisomer resulted from endoperoxidation across the unsubstituted central ring. We attribute this selectivity to the electron-donating character of the ether substituents increasing the reactivity of the substituted ring. Similar effects occur during analogous oxidations of naphthalenes, 1,4-dimethyl and 1,4-dimethoxy derivatives of which show selective endoperoxidation across the substituted positions.^[14]

Kinetics of Oxidation with $^1\text{O}_2$

The reactivity of acenes with $^1\text{O}_2$ often determines their photochemical stability, which is relevant for optoelectronic applications that require oxidation-resistant materials, as well as their potential for use in $^1\text{O}_2$ -responsive materials, which require rapid rates of oxidation. We determined the relative reactivity of these molecules to $^1\text{O}_2$ by irradiating MB (0.014 mM and $A_{654} \sim 1.26$) in air-equilibrated CH_2Cl_2 and monitoring acene concentration as a function of irradiation time by UV/vis spectrophotometry. As described above for NMR experiments, we used a long-pass optical filter ($\lambda > 630$ nm) to prevent direct irradiation of the acenes. Figure 5 shows representative UV/vis spectra of these acenes (after subtraction of the absorbance spectrum of the MB sensitizer) as a function of irradiation time.

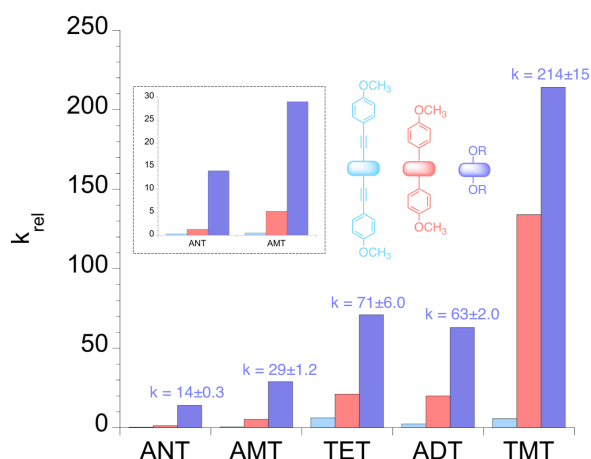


Figure 6. Comparison of the relative rate constants for dialkoxyacenes **2-6** (purple columns) to previously reported^[17] anisylethynyl (light blue columns) and anisyl derivatives (red columns). $k_{rel} = 1$ for 9,10-diphenylanthracene. ANT = Anthracene, AMT = Anthramonothiophene, TET = Tetracene, ADT = Anthradithiophene, TMT = Tetracenomonothiophene derivatives.

Using the assumption that the steady-state concentration of 1O_2 does not change during the irradiation experiment, we fit the kinetics of acene oxidation to pseudo first-order kinetics. Figure 6 shows rate constants of oxidation of these compounds relative to a commonly used standard for 1O_2 reactivity, 9,10-diphenylanthracene (DPA). Longer dialkoxyacenes reacted faster than shorter analogs, with effects of additional fused rings on kinetics of oxidation similar to those regarding spectroscopy described above. Using anthracene (ANT) **2** as a point of comparison, addition of a fused thiophene ring to the acene resulted in a smaller increase in reaction rate ($k_3 = 2k_2$) than addition of a fused benzene ring ($k_4 = 5k_2$), while addition of two thiophene rings had approximately the same effect as a fused benzene ring ($k_5 = 4.5k_2$). Tetracenomonothiophene (TMT) derivative **6**, which bears both an additional benzene ring and thiophene ring compared to **2**, reacted fastest with 1O_2 . In an effort to build consistent and generally applicable structure-property trends of acene reactivity, Figure 6 compares the relative rates of dialkoxyacenes **2-6** to previously reported analogs substituted in the same positions with either aryl groups or arylethynyl groups. For each of the five acene cores, the dialkoxy derivative reacted the fastest, while the diethynyl derivative reacted slowest. Moreover, the trend in reactivity as a function of acene core followed the same overall pattern as these previously reported examples, with the TMT derivative **6** emerging as a particularly reactive yet isolable acene, its reactivity enhanced by the combination of electron donating alkoxy groups and five linearly fused arenes.

Acid-promoted cleavage of dialkoxytetracene 4. The endoperoxides of alkoxyacenes present the unique structural feature of labile acetal-type linkages at endoperoxide bridgeheads. Previous studies have indicated that endoperoxides of these linkages in alkoxy-substituted naphthalenes and anthracene can fragment, especially under acidic conditions, to yield the corresponding quinone and

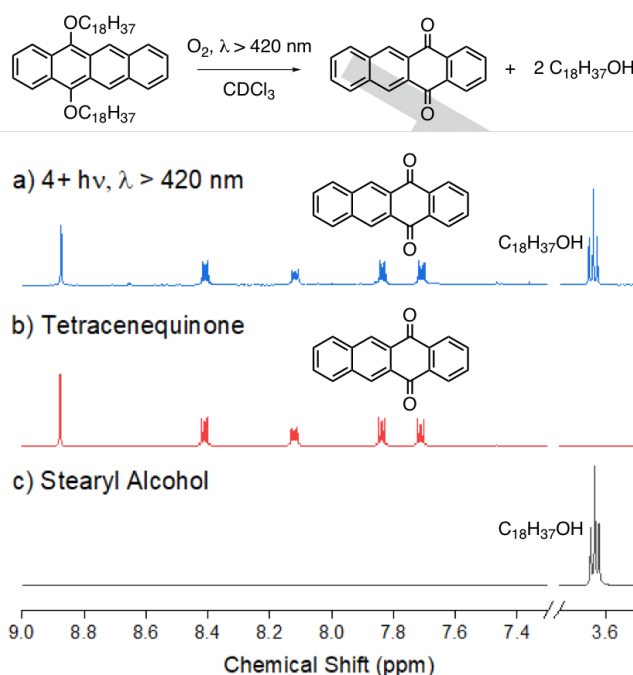


Figure 7. 1H NMR spectra in $CDCl_3$ of a) dialkoxytetracene **4** after 4 hours irradiation at $\lambda > 420$ nm, b) tetracenequinone, and c) stearyl alcohol.

alcohols.^{[11b],[14]} Given that such reactions break the ethereal C-O bonds in the starting acene, these downstream reactions of endoperoxides, as well as other 1O_2 -cleavable linkers, have proven useful in degradable materials and linkages, including for drug delivery.^{[11a,c],[19]}

Given the faster endoperoxidation of longer acenes demonstrated above, we sought to determine whether acenes with more than three fused rings—in particular we investigated dialkoxytetracene **4**—were susceptible to similar reactions. In addition to experiment employing an external photosensitizer described, we also irradiated tetracene **4** directly ($\lambda > 495$ nm in $CDCl_3$ in the absence of MB). This direct irradiation gave NMR spectra indistinguishable from those in which MB was irradiated. Therefore, at this concentration (6 mM) in aerated $CDCl_3$, we observed no [4+4] “butterfly” dimerization products.

We found that although the endoperoxide of **4** persisted in organic solvent, under mildly acidic conditions it fragmented upon irradiation with violet light. In particular, irradiation of **4** with $\lambda > 420$ nm in $CDCl_3$ which is known to contain HCl as an impurity, forms tetracenequinone and stearyl alcohol after 16 hours, as shown in the NMR spectra in Figure 7. The result bears some similarities to those Briseno and coworkers, who recently reported an acid-promoted rearrangement of rubrene endoperoxide in chlorinated solvents.^[23] Other experiments indicate that the tetracene endoperoxide of **4** is an intermediate to this cleavage reaction: i) stopping the direct irradiation after one hour yields endoperoxide as the only observed product, and ii) endoperoxide initially formed by irradiation using methylene blue sensitizer and $\lambda > 630$ nm could be fragmented to the same products (quinone and alcohol) by irradiating with $\lambda > 420$ nm. Additional experiments underscore the importance of acid in promoting this photoinduced cleavage: i) identical irradiation experiments in non-chlorinated solvents such as THF- d_6 or C_6D_6

gave only the endoperoxide as product, while addition of aqueous HCl to the C₆D₆ solution of **4** caused the photoinduced cleavage, and ii) addition of solid K₂CO₃ to the CDCl₃ solution prevented photoinduced cleavage under otherwise identical conditions. These observations suggest that longer, more oxidatively labile acenes have potential for degradable materials in acidic environments.

Conclusions

Although acenes hold a central position in organic optoelectronic materials, substituent patterns of long acenes with more than three fused rings are generally quite restricted, focusing primarily on the highly stable ethynyl derivatives. In contrast, this new family of dialkoxy-substituted acenes and thienoacenes reacts faster with ¹O₂ than even the corresponding aryl-substituted analogs of identical acene core structure. The optical spectra of these dialkoxyacenes is reliably red-shifted compared to analogous diarylacenes previously reported by our group.^[17] Moreover, the susceptibility of the acetal-endoperoxide products of these oxidations to photo-induced cleavage in acidic conditions and with visible light opens the possibility of using such acenes as photocleavable linkers for applications in degradable materials such as payload delivery. Taken together, this systematic investigation both enhances our fundamental understanding of how structure influences the optical and chemical reactivity properties of long acenes, but also suggests that alkoxyacenes are promising candidates for materials that respond to ¹O₂ for applications in either analytical measurements or selectively degradable materials.

Experimental Section

General Information

¹H and ¹³C NMR experiments were performed on a Bruker AVANCEIII 500 MHz NMR in deuterated solvent at room temperature. Chemical shifts are given in parts per million (ppm). All spectra were processed with Topspin 2.1 (Bruker Biospin). High-resolution mass spectral (HRMS) analyses of new compounds were performed by the Massachusetts Institute of Technology mass spectrometry facility and by the University of Illinois at Urbana-Champaign mass spectrometry laboratory, using electrospray ionization in positive mode.

All reactions were monitored using silica gel 60 F254 analytical TLC plates with UV detection ($\lambda = 254$ nm and 365 nm). Silica gel (60 Å, 40–63 μ m) and neutral aluminum oxide were used as the stationary phases for column chromatography. The optical spectra of compounds were measured in solvents of spectrophotometric quality. UV-vis absorption spectra were recorded using a Varian Cary-100 spectrophotometer in double beam mode. Fluorescence spectra were collected with a PTI Quantum Master 4 equipped with a 75 W Xe lamp. Fluorescence quantum yields were determined relative to either (i) anthracene in ethanol^[24] for compound **1** (ii) 9,10-diphenylanthracene in cyclohexane^[25] for compound **2** (iii) coumarin 6 in ethanol^[26] for compound **3** (iv) rhodamine 6G in ethanol^[25] for compounds **4**, **5**, and **6**. Time-resolved fluorescence data was collected under ambient conditions using a time-correlated single-photon counting instrument with a pulsed LED operating at 403 nm.

Irradiation experiments were performed with a 200 W Hg/Xe lamp (Newport-Oriel) equipped with a water filter, manual shutter, focusing lens, and the appropriate wavelength selecting filters. For irradiation at $\lambda > 630$ nm, a 630 nm long-pass filter was used, giving an average power density of 50.2 mW/cm². For irradiation at $\lambda > 495$ nm, two 495 nm long-pass filters were used in series, giving an average power density of 71 mW/cm². For irradiation at $\lambda > 420$ nm, two 420 nm long-pass filters were used in series, giving an average power density of 63 mW/cm².

Time-Dependent Density Functional Theory calculations were carried out using the ω B97x-D functional^[27] using the Tamm-Dancoff approximation at the 6-311+G(d,p) level of theory using atomic coordinates derived from geometry optimized coordinates beginning in a planar configuration. Geometry optimizations were executed on constructed atomic coordinates using the B3LYP functional at the 6-31G(d,p) level of theory. Time-dependent calculations were performed for the first 40 excited states. Displayed tables of results (see Supporting Information) include calculated molecular orbitals from HOMO-2 to LUMO+2 and the first 10 excited states, describing transitions with a 10% or greater contribution to the excited state. All DFT calculations were carried out using the Gaussian 09 software package.^[28]

Chemicals

All starting materials and solvents were purchased from Sigma-Aldrich, TCI Chemicals, or Fisher Scientific and, unless otherwise specified, were used without further purification. Deuterated solvents were purchased from Cambridge Isotope Laboratories.

Anthra[2,3-b]thiophene-5,10-dione,^[29] anthra[2,3-b:7,6-b']dithiophene-5,11-dione/Anthra[2,3-b:6,7-b']dithiophene-5,11-dione^[30] and tetraceno[2,3-b]thiophene-5,12-dione (TMT quinone)^[29] were synthesized according to literature procedures. Compounds **1-6** were stored in the dark under argon. Syntheses and handling of **4**, **5**, and **6** was performed in the dark.

Endoperoxide Formation

Irradiation at $\lambda > 630$ nm: ~ 5 mg of acene was dissolved in 1 mL of CDCl₃ and a small amount of methylene blue was added. The solution was irradiated at $\lambda > 630$ nm for one hour. The solution was oxygenated by sparging with air during the irradiation.

Direct irradiation of acene **4**: ~ 5 mg of acene **4** were dissolved in 1 mL of CDCl₃ and the solution was irradiated at $\lambda > 495$ nm for one hour. The solution was oxygenated by sparging with air during the irradiation.

Synthesis of **1**

Benzo[1,2-b:4,5-b']dithiophene-4,8-dione (0.20 g, 0.9 mmol), sodium dithionite (0.32 g, 1.8 mmol) and Adogen 464 (0.3 mL) were dissolved in a mixture of water (25 mL) and CH₂Cl₂ (25 mL) deoxygenated by sparging with argon and stirred for 5 minutes. After the addition of NaOH (0.36 g, 9.1 mmol), the mixture was stirred for ten more minutes. 1-Bromooctadecane (1.5 g, 4.5 mmol) was added portionwise, and the reaction mixture was allowed to stir at room temperature overnight. After separating the organic from the aqueous phase, the aqueous phase was extracted with CH₂Cl₂ (3 x 20 mL). The organic layers were combined, washed with water (3 x 20 mL), dried over MgSO₄ and filtered through a plug of silica. The solvent was removed *in vacuo* and the yellow crude product obtained was purified by flash column chromatography (SiO₂, gradient from hexanes to hexanes:CH₂Cl₂ = 7:1) to give 0.14 g of a white solid (yield = 21%).

¹H NMR (500 MHz, CDCl₃) δ 7.48 (d, $J = 5.5$ Hz, 2H), 7.36 (d, $J = 5.5$ Hz, 2H), 4.27 (t, $J = 6.6$ Hz, 4H), 1.90 – 1.84 (m, 4H), 1.59 – 1.52 (m, 4H), 1.41 – 1.29 (m, 56H), 0.88 (t, $J = 6.8$ Hz, 6H).

^{13}C NMR (126 MHz, CDCl_3) δ 144.7, 131.8, 130.3, 126.1, 120.5, 74.1, 32.1, 30.7, 29.9, 29.8, 29.8, 29.6, 29.5, 26.2, 22.9, 14.3.

HRMS (ESI+) m/z : $[\text{M}+\text{H}]^+$ Calcd for $\text{C}_{46}\text{H}_{79}\text{O}_2\text{S}_2$ 727.5521; Found 727.5524.

Synthesis of 2

9,10-Anthraquinone (0.13 g, 0.62 mmol), sodium dithionite (0.22 g, 1.2 mmol) and Adogen 464 (0.2 mL) were dissolved in a mixture of water (7.5 mL) and CH_2Cl_2 (7.5 mL) that was deoxygenated by sparging with Ar and stirred for 5 minutes. After the addition of NaOH (0.25 g, 6.2 mmol), the mixture was stirred for ten more minutes. 1-Bromooctadecane (1.03 g, 0.31 mmol) was added portionwise, and the reaction mixture was allowed to stir at room temperature overnight. After separating the organic and the aqueous phases, the aqueous phase was extracted with CH_2Cl_2 (3 x 20 mL). The organic layers were combined, washed with water (3 x 20 mL), dried over MgSO_4 and filtered through a plug of silica. The solvent was removed *in vacuo* and the yellow crude product obtained was purified by flash column chromatography (SiO_2 , gradient from hexanes to hexanes: CH_2Cl_2 = 7:1) to give 0.12 g of a light yellow solid (yield = 27%).

^1H NMR (500 MHz, CDCl_3) δ 8.29 – 8.27 (m, 4H), 7.48 – 7.46 (m, 4H), 4.15 (t, J = 6.7 Hz, 4H), 2.07 – 2.01 (m, 4H), 1.68 – 1.62 (m, 4H), 1.48 – 1.23 (m, 56H), 0.88 (t, J = 6.9 Hz, 6H).

^{13}C NMR (126 MHz, CDCl_3) δ 147.7, 125.3, 125.2, 122.9, 76.3, 32.1, 30.8, 29.9, 29.8, 29.8, 29.5, 26.4, 22.8, 14.3.

HRMS (ESI+) m/z : $[\text{M}+\text{H}]^+$ Calcd for $\text{C}_{50}\text{H}_{83}\text{O}_2$ 715.6393; Found 715.6415.

Synthesis of 3

Anthra[2,3-b]thiophene-5,10-dione (0.20 g, 0.76 mmol), sodium dithionite (0.26 g, 1.5 mmol) and Adogen 464 (0.4 mL) were dissolved in a mixture of water (15 mL) and CH_2Cl_2 (15 mL) deoxygenated by sparging with argon and stirred for 5 minutes. After the addition of NaOH (0.30 g, 7.6 mmol), the mixture was stirred for ten more minutes. 1-Bromooctadecane (1.3 g, 3.9 mmol) was added portionwise, and the reaction mixture was allowed to stir at room temperature overnight. After separating the organic and aqueous phases, the aqueous phase was extracted with CH_2Cl_2 (3 x 20 mL). The organic layers were combined, washed with water (3 x 20 mL), dried over MgSO_4 and filtered through a plug of silica. The solvent was removed *in vacuo* and the yellow crude product obtained was purified by flash column chromatography (SiO_2 , gradient from hexanes to hexanes: CH_2Cl_2 = 4:1) to give 0.12 g of a bright yellow solid (yield = 21%).

^1H NMR (500 MHz, CDCl_3) δ 8.80 (s, 1H), 8.75 (s, 1H), 8.36 – 8.31 (m, 2H), 7.51 (d, J = 5.7, 1H), 7.46 – 7.41 (m, 3H), 4.21 (q, J = 6.7 Hz, 4H), 2.13 – 2.05 (m, 4H), 1.73 – 1.65 (m, 4H), 1.51 – 1.21 (m, 56H), 0.88 (t, J = 6.9 Hz, 6H).

^{13}C NMR (126 MHz, CDCl_3) δ 148.0, 146.6, 139.1, 138.3, 129.1, 125.0, 124.8, 124.5, 124.1, 123.9, 123.9, 123.8, 122.9, 122.8, 116.9, 115.7, 76.4, 76.3, 30.9, 30.9, 29.9, 29.8, 29.8, 29.5, 26.5, 26.4, 22.9, 14.3.

HRMS (ESI+) m/z : $[\text{M}]^+$ Calcd for $\text{C}_{52}\text{H}_{82}\text{O}_2\text{S}$ 770.6030; Found 770.6022.

Synthesis of 4

5,12-Naphthacenequinone (0.20 g, 0.77 mmol), sodium dithionite (0.27 g, 1.6 mmol) and Adogen 464 (0.3 mL) were dissolved in a mixture of water (7.5 mL) and CH_2Cl_2 (7.5 mL) deoxygenated by sparging with argon and stirred for 5 minutes. After the addition of NaOH (0.31 g, 7.7 mmol), the mixture was stirred for ten more minutes. 1-Bromooctadecane (1.3 g, 3.9 mmol) was added portionwise, and the reaction mixture was allowed to

stir at room temperature overnight. After separating the organic and aqueous phases, the aqueous phase was extracted with CH_2Cl_2 (3 x 20 mL). The organic layers were combined, washed with water (3 x 20 mL), dried over MgSO_4 and filtered through a plug of silica. The solvent was removed *in vacuo* and the orange crude product obtained was purified by flash column chromatography (SiO_2 , gradient from hexanes to hexanes: CH_2Cl_2 = 85:15) to give 0.28 g of a bright orange solid (yield = 48%).

^1H NMR (500 MHz, CDCl_3) δ 8.90 (s, 2H), 8.29 – 8.25 (m, 2H), 8.05 – 8.01 (m, 2H), 7.43 – 7.37 (m, 4H), 4.26 (t, J = 6.7 Hz, 4H), 2.15 – 2.09 (m, 4H), 1.75 – 1.68 (m, 4H), 1.52 – 1.22 (m, 56H), 0.88 (t, J = 6.9 Hz, 6H).

^{13}C NMR (126 MHz, CDCl_3) δ 147.7, 131.4, 128.8, 125.5, 124.9, 124.8, 124.1, 122.9, 121.6, 76.4, 32.1, 30.9, 29.9, 29.8, 29.5, 26.5, 22.9, 14.3.

HRMS (ESI+) m/z : $[\text{M}+\text{H}]^+$ Calcd for $\text{C}_{54}\text{H}_{85}\text{O}_2$ 765.6550; Found 765.6563.

Synthesis of 5

Anthra[2,3-b:7,6-b']dithiophene-5,11-dione/Anthra[2,3-b:6,7-b']dithiophene-5,11-dione (0.10 g, 0.31 mmol), sodium dithionite (0.11 g, 0.63 mmol) and Adogen 464 (0.2 mL) were dissolved in a mixture of water (7.5 mL) and CH_2Cl_2 (7.5 mL) deoxygenated by sparging with argon and stirred for 5 minutes. After the addition of NaOH (0.125 g, 3.1 mmol), the mixture was stirred for ten more minutes. 1-Bromooctadecane (0.523 g, 1.6 mmol) was added portionwise, and the reaction mixture was allowed to stir at room temperature overnight. After separating the organic and aqueous phases, the aqueous phase was extracted with CH_2Cl_2 (3 x 20 mL). The organic layers were combined, washed with water (3 x 20 mL), dried over MgSO_4 and filtered through a plug of silica. The solvent was removed *in vacuo* and the red crude product obtained was purified by flash column chromatography (SiO_2 , gradient from hexanes to hexanes: CH_2Cl_2 = 4:1) to give 0.054 g of a red solid (yield = 21%).

^1H NMR (500 MHz, CDCl_3) δ 8.80 (s, 2H), 8.75 (s, 2H), 7.50 – 7.47 (m, 2H), 7.40 (d, J = 5.6 Hz, 2H), 4.26 (quin, J = 6.5 Hz, 4H), 2.18 – 2.09 (m, 4H), 1.78 – 1.68 (m, 4H), 1.52 – 1.21 (m, 56H), 0.88 (t, J = 6.9 Hz, 6H).

^{13}C NMR (126 MHz, CDCl_3) δ 148.3, 146.9, 145.5, 139.0, 138.9, 138.1, 137.9, 129.2, 129.1, 123.9, 123.2, 123.1, 122.9, 122.8, 116.8, 116.8, 115.5, 115.5, 76.4, 76.4, 76.3, 32.1, 31.0, 29.9, 29.8, 29.5, 26.5, 22.9, 14.3.

HRMS (ESI+) m/z : $[\text{M}+\text{H}]^+$ Calcd for $\text{C}_{54}\text{H}_{83}\text{O}_2\text{S}_2$ 827.5834; Found 827.5786.

Synthesis of 6

Tetraceno[2,3-b]thiophene-5,12-dione (0.160 g, 0.51 mmol), sodium dithionite (0.177 g, 1.0 mmol) and tetrabutylammonium bromide (0.082 g, 0.25 mmol) were dissolved in a mixture of water (10 mL) and THF (20 mL) deoxygenated by sparging with argon and stirred for 5 minutes. After the addition of KOH (0.285 g, 5.1 mmol), the mixture was stirred for fifteen more minutes. Dimethyl sulfate (0.24 mL, 2.5 mmol) was added dropwise, and the reaction mixture was allowed to stir at room temperature overnight. After separating the organic and aqueous phases, the aqueous phase was extracted with EtOAc (3 x 20 mL). The organic layers were combined, washed with water (3 x 20 mL), dried over Na_2SO_4 and filtered. The solvent was removed *in vacuo* and the purple crude product obtained was purified by gravity column chromatography (Aluminum oxide, hexanes:EtOAc = 95:5) to give 8 mg of a purple solid (yield = 5%).

^1H NMR (500 MHz, δ) 8.96 (s, 2H), 8.85 (s, 1H), 8.79 (s, 1H), 8.05 – 8.03 (m, 2H), 7.61 (d, $J = 5.5$, 1H), 7.45 (d, $J = 5.5$, 1H), 7.37 – 7.35 (m, 2H), 4.25 (d, $J = 4$, 6H).

^{13}C NMR (126 MHz, CDCl_3) δ 149.6, 148.2, 140.2, 139.0, 132.2, 132.1, 130.3, 129.3, 129.2, 126.0, 125.9, 124.3, 124.0, 123.3, 123.2, 121.8, 121.7, 117.1, 115.7, 63.3, 63.3.

HRMS (ESI+) m/z : $[\text{M}+\text{H}]^+$ Calcd for $\text{C}_{22}\text{H}_{17}\text{O}_2\text{S}$ 345.0949; Found 345.0934.

Acknowledgements

We gratefully acknowledge the NSF (CHE-1609146) for generous support of this work. We thank Professor Samer Gozem (Georgia State University) for his assistance with TD-DFT calculations.

Keywords: Acenes • Organic Synthesis • Singlet Oxygen • Endoperoxide • Fluorescence

- [1] a) C. Wang, H. Dong, W. Hu, Y. Liu, D. Zhu, *Chem. Rev.* **2012**, *112*, 2208–2267; b) A. Naibi Lakshminarayana, A. Ong, C. Chi, *J. Mater. Chem. C* **2018**, *6*, 3551–3563.
- [2] a) J. E. Anthony, *Chem. Rev.* **2006**, *106*, 5028–5048; b) H. D. Pham, H. Hu, F.-L. Wong, C.-S. Lee, W.-C. Chen, K. Feron, S. Manzhos, H. Wang, N. Motta, Y. M. Lam, et al., *J. Mater. Chem. C* **2018**, *6*, 9017–9029.
- [3] Y. Lim, S.-G. Ihn, X. Bulliard, S. Yun, Y. Chung, Y. Kim, H. Chang, Y. S. Choi, *Polymer* **2012**, *53*, 5275–5284.
- [4] a) S. S. Zade, N. Zamoshchik, A. R. Reddy, G. Fridman-Marueli, D. Sherberla, M. Bendikov, *J. Am. Chem. Soc.* **2011**, *133*, 10803–10816; b) J. Reichwagen, H. Hopf, A. Del Guerzo, J.-P. Desvergne, H. Bouas-Laurent, *Org. Lett.* **2004**, *6*, 1899–1902.
- [5] a) J.-F. Xu, Y.-Z. Chen, L. Z. Wu, C.-H. Tung, Q.-Z. Yang, *Org. Lett.* **2013**, *15*, 6148–6151. b) Y.-L. Liu, T.-W. Chuo, *Polym. Chem.* **2013**, *4*, 2194–2205. c) H. Sun, C. P. Kabb, Y. Dai, M. R. Hill, I. Ghiviriga, A. P. Bapat, B. S. Sumerlin, *Nat. Chem.* **2017**, *9*, 817–823. d) B. C. Popere, G. E. Sanoja, E. M. Thomas, N. S. Schausser, S. D. Jones, J. M. Bartels, M. E. Helgeson, M. L. Chabinyr, R. A. Segalman, *J. Mater. Chem. C* **2018**, *6*, 8762–8769.
- [6] a) S. Kim, M. Fujitsuka, T. Majima, *J. Phys. Chem. B* **2013**, *117*, 13985–13992. b) S. K. Petersen, J. Holmehave, F. H. Blaikie, A. Gollmer, T. Breitenbach, H. H. Jensen, P. R. Ogilby, *J. Org. Chem.* **2014**, *79*, 3079–3087. c) K. Tanaka, T. Miura, N. Umezawa, Y. Urano, K. Kikuchi, T. Higuchi, T. Nagano, *J. Am. Chem. Soc.* **2001**, *123*, 2530–2536. d) S. W. Thomas III, E. Altinok, J. Zhang *Synlett* **2016**, *27*, 355–368.
- [7] a) F. Frausto, S. W. Thomas, *ACS Appl. Mater. Interfaces* **2017**, *9*, 15768–15775; b) F. Frausto, S. W. Thomas, *ChemPhotoChem* **2018**, *2*, 632–639.
- [8] A. A. Ghogare, A. Greer, *Chem. Rev.* **116**, 9994–10034.
- [9] a) W. Fudickar, T. Linker, *Chem. - Eur. J.* **2011**, *17*, 13661–13664; b) W. Fudickar, T. Linker, *J. Org. Chem.* **2017**, *82*, 9258–9262.
- [10] a) S. Kolemen, T. Ozdemir, D. Lee, G. M. Kim, T. Karatas, J. Yoon, E. U. Akkaya, *Angew. Chem. Int. Ed.* **2016**, *55*, 3606–3610; *Angew. Chem.* **2016**, *128*, 3670–3674; b) W. Fudickar, T. Linker, *Angew. Chem. Int. Ed.* **2018**, *57*, 12971–12975; *Angew. Chem.* **2018**, *130*, 13153–13157.
- [11] a) D. Arian, L. Kovbasyuk, A. Mokhir, *J. Am. Chem. Soc.* **2011**, *133*, 3972–3980; b) M. Bauch, M. Klaper, T. Linker, *J. Phys. Org. Chem.* **2017**, *30*, e3607; c) V. Brega, F. Scaletti, X. Zhang, L.-S. Wang, P. Li, Q. Xu, V. M. Rotello, S. W. Thomas, *ACS Appl. Mater. Interfaces* **2019**, *11*, 2814–2820.
- [12] B. Stevens, S. R. Perez, J. A. Ors, *J. Am. Chem. Soc.* **1974**, *96*, 6846–6850.
- [13] C. Pierlot, J. Poprawski, J. Marko, J.-M. Aubry, *Tetrahedron Lett.* **2000**, *41*, 5063–5067.
- [14] M. Bauch, A. Kritischka, T. Linker, *J. Phys. Org. Chem.* **2017**, *30*, e3734.
- [15] S. S. Palayangoda, R. Mondal, B. K. Shah, D. C. Neckers, *J. Org. Chem.* **2007**, *72*, 6584–6587.
- [16] J. Schwaben, N. Münster, T. Breuer, M. Klues, K. Harms, G. Witte, U. Koert, *Eur. J. Org. Chem.* **2013**, *2013*, 1639–1643.
- [17] J. Zhang, Z. C. Smith, S. W. Thomas, *J. Org. Chem.* **2014**, *79*, 10081–10093.
- [18] M. Mamada, H. Katagiri, M. Mizukami, K. Honda, T. Minamiki, R. Teraoka, T. Uemura, S. Tokito, *ACS Appl. Mater. Interfaces* **2013**, *5*, 9670–9677.
- [19] a) S. P. Patil, B. A. Moosa, S. Alsaiani, K. Alamoudi, A. Alshamsan, A. AlMalik, K. Adil, M. Eddaoudi, N. M. Khashab, *Chem. - Eur. J.* **2016**, *22*, 13789–13793; b) Q. Yan, J. Hu, R. Zhou, Y. Ju, Y. Yin, J. Yuan, *Chem. Commun.* **2012**, *48*, 191; c) T. Qian, F. Chen, Y. Chen, Y.-X. Wang, W. Hu, *Chem Commun* **2017**, *53*, 11822–11825. d) G. Ghosh, S. J. Belh, C. Chiemezie, N. Walalawela, A. A. Ghogare, M. Vignoni, A. H. Thomas, S. A. McFarland, E. M. Greer, A. Greer *Photochem. Photobiol.* **2019**, *95*, 293–305.
- [20] K. I. Salokhiddinov, I. M. Byteva, G. P. Gurinovich, *J. Appl. Spectrosc.* **1981**, *34*, 561–564.
- [21] a) B. McDearmon, E. Lim, I.-H. Lee, L. M. Kozyc, K. O'Hara, P. I. Robledo, N. R. Venkatesan, M. L. Chabinyr, C. J. Hawker, *Macromolecules* **2018**, *51*, 2580–2590; b) B. McDearmon, Z. A. Page, M. L. Chabinyr, C. J. Hawker, *J. Mater. Chem. C* **2018**, *6*, 3564–3572.
- [22] R. N. Baral, S. W. Thomas, *J. Org. Chem.* **2015**, *80*, 11086–11091.
- [23] J. T. Ly, S. A. Lopez, J. B. Lin, J. J. Kim, H. Lee, E. K. Burnett, L. Zhang, A. Aspuru-Guzik, K. N. Houk, A. L. Briseno, *J. Mater. Chem. C* **2018**, *6*, 3757–3761.
- [24] W. H. Melhuish, *J. Phys. Chem.* **1961**, *65*, 229–235.
- [25] J. R. Lakowicz, *Principles of Fluorescence Spectroscopy*, Springer, New York, NY, **2010**.
- [26] K. H. Drexhage, *J. Res. Natl. Bur. Stand., Sect. A* **1976**, *80*, 421–428.
- [27] J.-D. Chai, M. Head-Gordon, *Phys. Chem. Chem. Phys.* **2008**, *10*, 6615–6620.
- [28] Gaussian 09, Revision D.01, M. J. Frisch, G. W. Trucks, H. B. Schlegel, G. E. Scuseria, M. A. Robb, J. R. Cheeseman, G. Scalmani, V. Barone, G. A. Petersson, H. Nakatsuji, X. Li, M. Caricato, A. Marenich, J. Bloino, B. G. Janesko, R. Gomperts, B. Mennucci, H. P. Hratchian, J. V. Ortiz, A. F. Izmaylov, J. L. Sonnenberg, D. Williams-Young, F. Ding, F. Lipparini, F. Egidi, J. Goings, B. Peng, A. Petrone, T. Henderson, D. Ranasinghe, V. G. Zakrzewski, J. Gao, N. Rega, G. Zheng, W. Liang, M. Hada, M. Ehara, K. Toyota, R. Fukuda, J. Hasegawa, M. Ishida, T. Nakajima, Y. Honda, O. Kitao, H. Nakai, T. Vreven, K. Throssell, J. A. Montgomery, Jr., J. E. Peralta, F. Ogliaro, M. Bearpark, J. J. Heyd, E. Brothers, K. N. Kudin, V. N. Staroverov, T. Keith, R. Kobayashi, J. Normand, K. Raghavachari, A. Rendell, J. C. Burant, S. S. Iyengar, J. Tomasi, M. Cossi, J. M. Millam, M. Klene, C. Adamo, R. Cammi, J. W. Ochterski, R. L. Martin, K. Morokuma, O. Farkas, J. B. Foresman, and D. J. Fox, Gaussian, Inc., Wallingford CT, **2016**.
- [29] F. Valiyeu, W.-S. Hu, H.-Y. Chen, M.-Y. Kuo, I. Chao, Y.-T. Tao, *Chem. Mater.* **2007**, *19*, 3018–3026.
- [30] L. Chen, S. R. Puniredd, Y.-Z. Tan, M. Baumgarten, U. Zschieschang, V. Enkelmann, W. Pisula, X. Feng, H. Klauk, K. Müllen, *J. Am. Chem. Soc.* **2012**, *134*, 17869–17872.

FULL PAPER

Dialkoxyacenes with three or more fused rings react rapidly with singlet oxygen ($^1\text{O}_2$) to yield endoperoxides, with potential applications in $^1\text{O}_2$ detection or degradable materials.



Valentina Brega, Sare Nur Kanari,
Connor T. Doherty, Dante Che, Seth
A. Sharber, and Samuel W. Thomas
III*

Page No. – Page No.

Spectroscopy and Reactivity of
Dialkoxy Acenes